Photodiagnosis and Photodynamic Therapy 37 (2022) 102652

Contents lists available at ScienceDirect

Photodiagnosis and Photodynamic Therapy

journal homepage: www.elsevier.com/locate/pdpdt

Original article

Factors effecting the choroidal vascularity index in children with mild to moderate myopia

Nazife Aşıkgarip [a], Emine Temel [a,*], Kemal Örnek [b]

[a] Kırşehir Ahi Evran Training and Research Hospital, Department of Ophthalmology, Kırşehir, Turkey
[b] Kırşehir Ahi Evran University School of Medicine, Department of Ophthalmology, Kırşehir, Turkey

ARTICLE INFO

Keywords:
Binarization
Choroidal area
Choroidal vascularity index
Myopia
Pediatric population
Optical Coherence Tomography

ABSTRACT

Purpose: To measure the choroidal structural parameters in a population of myopic children and determine the factors effecting the choroidal vascularity index (CVI).

Methods: **:**In total, 200 eyes of 200 children (100 females, 100 males) with a mean age of 11.5 ± 1.6 years were included in the study. Macular imaging was performed using EDI mode of spectral domain-optical coherence tomography. Binarization of the choroidal area was performed with ImageJ software. Total choroidal area, luminal area (LA), stromal area (SA), and CVI were automatically calculated.

Results: The mean choroidal, stromal and luminal areas were measured as 0.952 ± 0.127 mm^2, 0.626 ± 0.103 mm^2 and 0.325 ± 0.076 mm^2, respectively. The mean CVI was 65.81% ± 6.56. Age and the axial length (AL) of the participants were not found to be associated with the LA and the CVI. (r=-0.078, p=0.274, r=0.017, p=0.808, and r=0,051, p=0.474 and r=-0.128, p=0.071, respectively). There was a statistically significant strong association between the LA and CVI measurements and SE of the participants (r=0.736, p=0.001, and r=-0.605; p=0.001).

Conclusion: Age and AL were not associated with the CVI, but SE was significantly associated with the CVI.

1. Introduction

Myopia is the most common refractive error that usually develops during childhood. The global prevalence has been reported to be as high as 80% in Asia and 22.9% in other parts of the world.[1–3] Therefore, it is critical to control the development and progression of myopia and investigate the underlying mechanisms of myopia that are not yet fully clarified ..

In addition to nourishing the retina, the choroid has an essential role in the refraction of the eye through the modulation of its thickness as shown by Wallman et al.[4] Moreover, it delivers retinal signals to the sclera to affect ocular size that leads to refraction changes.[5] A number of studies have demonstrated subfoveal choroidal thinning in patients with varying degrees of myopia.[6–19] There were significant associations between the choroidal thickness (CT) and age, refractive error, axial length (AL), and gender, in both adults and children.[9, 11, 14-19]

In recent years, the choroidal vascularity index (CVI) has been of great interest for researchers as an objective marker of the choroidal vasculature. Previous imaging techniques were limited to a two-dimensional visualization of the choroid, and only large vessels could be quantified.[20–23] The enhanced-depth imaging (EDI) optical coherence tomography (OCT) enabled the visualization of three-dimensional choroidal vasculature with more clear images.[24–27] To date, only two studies evaluated the choroidal structure and its associations in myopic school-aged children with conflicting results.[28,29]

In this study, our objective was to measure the choroidal structural parameters in a population of myopic children and determine the factors affecting the CVI.

2. Materials and methods

This prospective cross-sectional study included children recruited from the outpatient clinic of the Ophthalmology Department between February 2021 and June 2021. It was approved by the institutional review board and adhered to the tenets of the Declaration of Helsinki. A signed informed consent form was obtained from the parents of each participant.

The inclusion criteria were; age between 10 and 15 years, low to moderate myopia (spherical equivalent (SE) refraction at least − 1.00

* Corresponding author at: Department of Ophthalmology, Kırşehir Ahi Evran Training and Research Hospital.
E-mail address: emine912@hotmail.com (E. Temel).

https://doi.org/10.1016/j.pdpdt.2021.102652
Received 5 October 2021; Received in revised form 29 October 2021; Accepted 22 November 2021
Available online 24 November 2021
1572-1000/

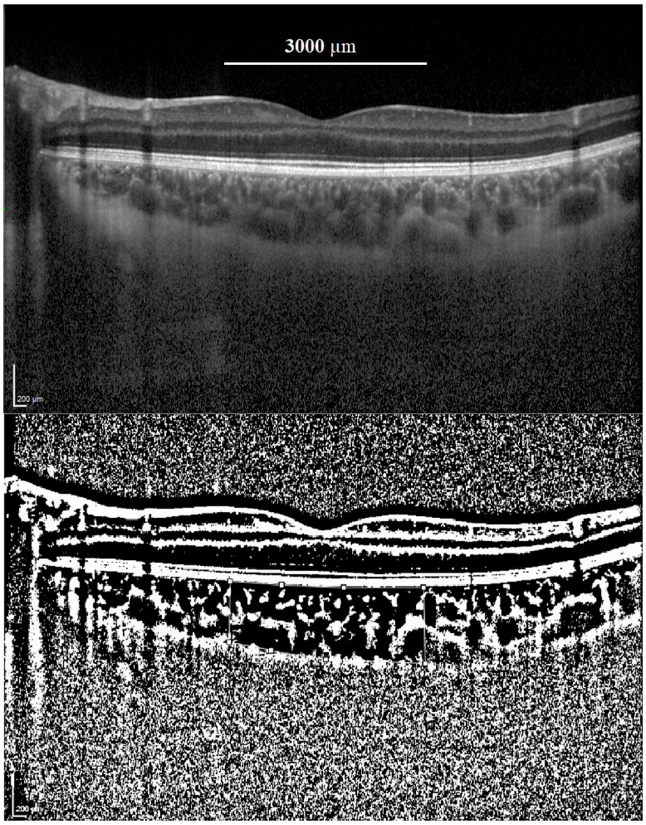

Fig. 1. Optical coherence tomographic images of choroid converted to binarization images. The area of interest of the choroid is demarcated (top). The image is converted to a binary image using ImageJ. The luminal area and the stromal area are visible (bottom).

diopter (D) and diopter of spherical within − 0.50 D to − 5.50 D in either eye), myopic astigmatism ≤ − 1.50 D and anisometropia of less than 1.50 D.

The exclusion criteria were as follows: best-corrected visual acuity (BCVA) < 20 / 25, high myopia; wearing contact lenses within 3 days of the examination, intraocular pressure (IOP) ≥ 21 mmHg, axial length (AL) < 22 mm and > 26 mm, history of any systemic disease as diabetes or hypertension; any ophthalmic disease, history of intraocular surgery, use of anticholinergic and cholinergic drugs.

Each participant underwent a complete ophthalmic examination, including measurement of BCVA, IOP using non-contact tonometry, refraction and AL, slit-lamp biomicroscopy and dilated fundoscopy.

Macular imaging was performed using EDI mode of spectral domain-OCT (software version 6.3.3.0, Heidelberg Engineering Inc., Heidelberg, Germany). The OCT device contains a superluminescent diode with a wavelength of 870 nm and could obtain 40.000 scans per second. The axial and transverse resolutions are 7 and 14 μm, respectively. Two high-quality horizontal line scans are obtained through the fovea using a 1 × 30-degree area. We averaged 100 scans for each section. The automatic real-time averaging mode that maximizes the signal-to-noise ratio was used to ensure high-quality images. In the EDI mode, the device moves closer to the patient to focus on the posterior part of the eye and observe the choroidal tissue more in detail. Eye tracking, EDI, and follow-up modes were enabled to reduce motion artifacts, enhance the visibility of the choroid and ensure a constant scanning area throughout all scans. Before recording the images, keratorefractive values of the subjects were entered into the software of the OCT device to estimate optical magnification. All OCT images were captured between 9:00 am and 12:00 pm under dim light conditions by the same technician after dilation of the pupils with topical 0.5% tropicamide.

Table 1
The demographic and clinical characteristics of the participants.

Participants / Eyes (n)	200 / 200
Age (years) (Range)	11.5 ± 1.6 (10-15)
Female / Male	100 / 100
Intraocular pressure (mmHg) (Range)	13.61 ± 2.23 (10-16)
Axial length (mm) (Range)	24.1 ± 1.08 (22.0-26.0)
Spherical equivalent (Range)	−2.68 ± 1.48 (− 0.50 to - 5.50)

The examined choroidal area was determined for a large 3000-μm-width area. After recording of the EDI-SD OCT images, the best image was displayed on a computer screen and evaluated by the 2 masked ophthalmologists (ET and NA) independently. The OCT scans with a signal strength of at least six or above and good reliability were included in the analysis. Only one eye per subject was selected. When the 2 ophthalmologists determined that the choroidal image was clearly distinguishable, the image was considered acceptable and used for the following analyses.

The upper margin of the region of interest (ROI) was the RPE line and the lower margin was the chorioscleral border in the EDI-SD OCT images. The nasal margin was the edge of the optic nerve head and the temporal margin was 3000 μm temporal from the edge of the optic nerve head. The distance was determined by the auto adjust function embedded in the OCT device.

Binarization of the choroidal area was performed with ImageJ (Version 1.50a, National Institutes of Health, Bethesda, Maryland, USA; available at imagej.nih.gov/ij/). An ROI was selected and set by the ROI manager in the OCT image. Then, three choroidal vessels with lumens larger than 100 μm were randomly selected by the oval selection tool of the tool bar, and the average reflectivity of these areas was determined by the software. The average brightness was set as the minimum value to minimize the noise in the OCT image. Then, the image was converted to 8 bits and adjusted by the auto local threshold of Niblack. The binarized image was reconverted to an RGB image, and the luminal area was determined using the threshold tool. After the data for the distance of each pixel were added, the total choroidal area, luminal area (LA), and stromal area (SA) were automatically calculated. The light pixels were defined as the stromal choroid or choroidal interstitial area and the dark pixels were defined as the luminal area. The CVI was calculated as the ratio between the LA and choroidal area. (Fig. 1)

NCSS (Number Cruncher Statistical System) 2007 (Kaysville, Utah, USA) program was used for statistical analysis. Descriptive statistical methods (mean, standard deviation) were used when evaluating study data. The conformity of the quantitative data to the normal distribution was tested with the Shapiro-Wilk test and graphical examinations. Linear logistic regression analysis was used in multivariate evaluations. Agreement between intra-observer and inter-observer measurements were assessed using the intraclass correlation coefficient. Statistical significance was evaluated at the 0.05 level.

3. Results

In total, 200 eyes of 200 children (100 females, 100 males) with a mean age of 11.5 ± 1.6 years were included in the study. The mean total AL was 24.1 ± 1.08 mm (ranging from 22 to 26 mm) and the mean total SE was − 2.68 ± 1.48 D (ranging from − 0.50 D to −5.50 D). The mean IOP was 13.61 ± 2.23 mmHg (ranging from 10 to 16 mmHg).

The demographic and clinical characteristics of the participants are listed in Table 1.

The mean choroidal, stromal and luminal areas were measured as 0.952 ± 0.127 mm^2, 0.626 ± 0.103 mm^2 and 0.325 ± 0.076 mm^2, respectively. The mean CVI was 65.81% ± 6.56.

The LA was 0,31±0,08 mm^2 in the female group and 0,34±0,07 mm^2 in the male group (p = 0,017). The CVI was significantly increased in female participants (0,67%±0,07) compared with male participants

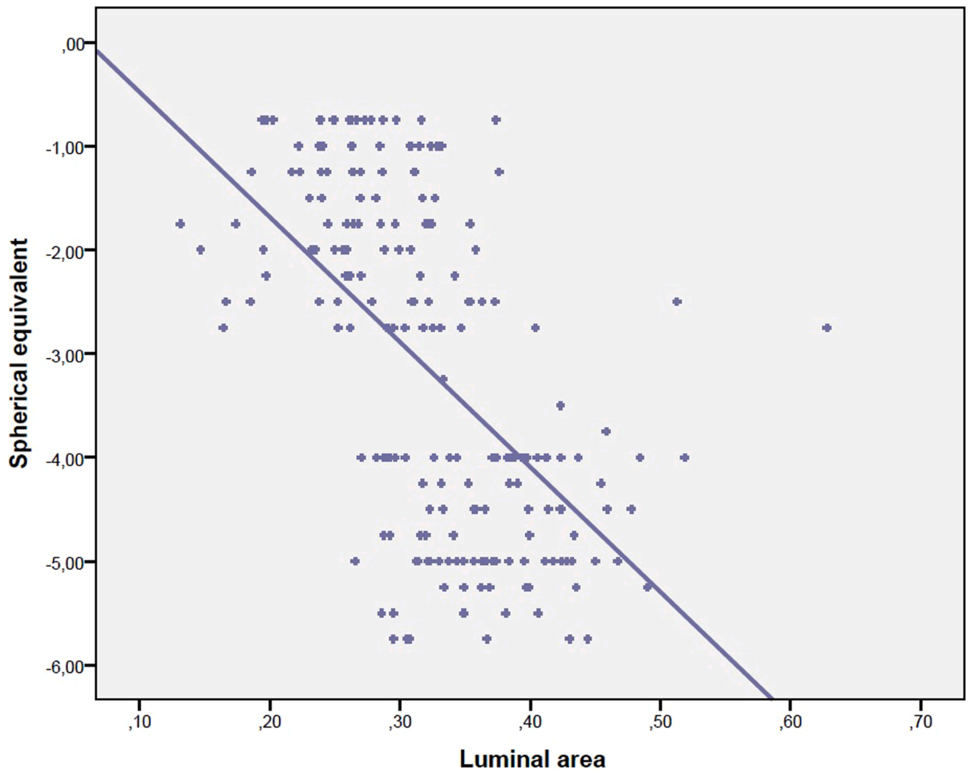

Fig. 2. There was a statistically significant strong association between the LA and SE of the participants (r=0.736, p=0.001).

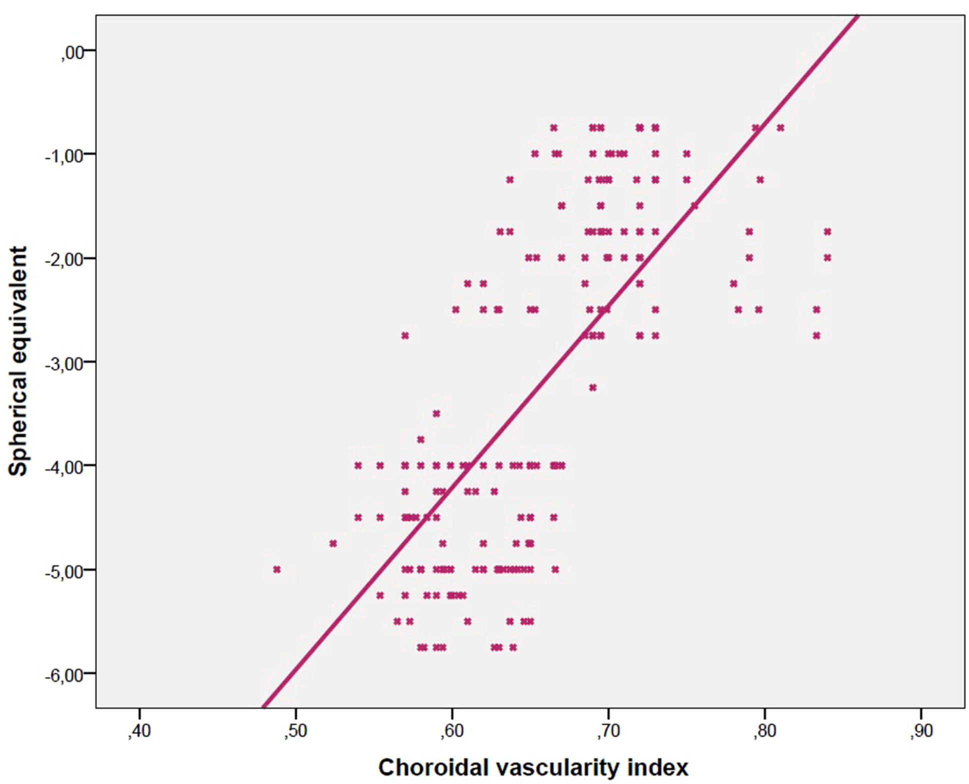

Fig. 3. There was a statistically significant strong association between the CVI and SE of the participants (r=-0.605; p=0.001).

(0,64% ± 0,06) (p = 0.001).

The age and AL of the participants were not associated with the LA and the CVI. (r = - 0.078, p = 0.274, r = 0.017, p = 0.808, and r = 0,051, p = 0.474 and r = - 0.128, p = 0.071, respectively).

There was a statistically significant strong association between the LA and CVI measurements and SE of the participants (r = 0.736, p = 0.001, and r= - 0.605; p = 0.001) (Figs. 2, 3).

A multiple regression analysis was performed to determine the

Table 2
Repeatability and reproducibility of all measurements.

	Cronbach's Alpha	Intraclass correlation coefficient	95% CI Lower	Upper
Choroidal area				
Repeatability Examiner 1	0.998	0.998	0.997	0.999
Repeatability Examiner 2	0.998	0.998	0.997	0.999
Reproducibility Examiner 1 versus Examiner 2	0.998	0.998	0.997	0.999
Luminal area				
Repeatability Examiner 1	0.997	0.997	0.995	0.998
Repeatability Examiner 2	0.998	0.998	0.997	0.999
Reproducibility Examiner 1 versus Examiner 2	0.998	9.998	0.997	0.999
Stromal area				
Repeatability Examiner 1	0.998	0.998	0.997	0.999
Repeatability Examiner 2	0.997	0.997	0.995	0.998
Reproducibility Examiner 1 versus Examiner 2	0.998	0.998	0.997	0.999
Choroidal vascularity index				
Repeatability Examiner 1	0.997	0.997	0.995	0.998
Repeatability Examiner 2	0.998	0.998	0.997	0.999
Reproducibility Examiner 1 versus Examiner 2	0.988	0.988	0.981	0.992

effects of the gender, the CVI, the choroidal area, and the SE measurements on the LA. We found that the choroidal area and SE had a significant effect on the LA (Table 2). Gender did not have a significant effect on the LA (p>0,05).

Backward regression analysis to determine the risk factors affecting the LA was statistically significant (F=8874,993; p=0.001; p<0.01). There was a relationship between the choroidal area and the CVI as the determinants of the LA. With these variables, the LA disclosure rate was 98.9%, which was at a strong level. While choroidal area value increased the luminal area (β: 0.611); CVI, on the other hand, decreased the LA (β:-0.943). Gender was not found to be effective on the LA (p>0.05).

A multiple regression analysis was performed to determine the effects of the gender, SA, LA, and SE measurements on the CVI. As a result of the analysis, it was found that the SA, LA, and SE measurements had a significant effect on the CVI (Table 3).

(Table 4)

Backward regression analysis to determine the risk factors affecting CVI measurements was statistically significant (F=4080,582; p=0.001; p<0.01). There was a relationship with the SA, LA, and SE as the determinants of the CVI measurements. The CVI disclosure rate with these variables was 98.4%, which was at a strong level. The SA and SE values increased the CVI (β: 0.357; β:0.002, respectively), and the LA decreased the CVI (β:-0.657). Gender was not found to be effective on the CVI (p>0.05).

When inter-observer reproducibility for all measurements between the 2 examiners was assessed, there was an excellent agreement. When the intra-observer repeatability was evaluated, all measurements were found to have high repeatability for both examiners. Repeatability and reproducibility of all measurements were shown in Table 2.

4. Discussion

The study demonstrated that the age and AL were not associated with the CVI in myopic children. There was a significant association between the CVI and SE of the participants. Gender did not reveal a significant effect on the CVI.

Positioned between the sclera and the retina, the highly vascularized choroid is essential for maintaining normal vision and ocular function. Besides these primary roles, it is also thought to play a critical role in the mechanisms underlying the control of ocular growth and the development of refractive errors like myopia· [4,29] Although the exact mechanisms of myopia development are unknown, growing evidence suggests that choroid may contribute to the myopic pathogenesis.

Several studies have shown the characteristics of choroidal thickness (CT) changes and the associated factors in myopic children. Choroidal thickness reflects the total choroidal vasculature without any distinctions between the stromal and luminal vascular components. In 2013, Branchini et al. firstly devised an automated software to calculate the area of dark and light pixels corresponding to luminal and stromal areas of the choroid· [30] Later, Sonoda et al. and Agrawal et al. improved the method using the EDI-OCT scans· [31,32] In the recent years, the CVI defined as the ratio of LA to total choroidal area, has been used as one of the biomarkers to evaluate the vascular status of the choroid. Previous reports have suggested the role of the CVI in various disease entities including central serous chorioretinopathy, polypoidal choroidal vasculopathy, panuveitis, Vogt-Koyanagi-Harada disease, and age-related macular degeneration· [33–37]

Read et al. measured the CT in myopic and non-myopic children and found that the refractive error and age were significantly associated with the subfoveal CT, with the refractive error appearing to be the stronger

Table 3
Linear Regression Analysis of Risk Factors Affecting Luminal Area

The dependent variable	Independent variable	ß	T	p	F	Model (p)	R^2
Luminal Area	Fixed	0,611	85,438	0,001**	8874,993	0,001	0,989
	Choroidal area	0,352	78,455	0,001**			
	CVI	-0,943	-108,209	0,001**			
***p < 0,01*							

Table 4
Linear Regression Analysis of Risk Factors Affecting CVI

The dependent variable	Independent variable	ß	T	p	F	Model (p)	R^2
CVI	Fixed	0,653	137,993	0,001**	4080,582	0,001	0,984
	Stromal area	0,357	55,020	0,001**			
	Luminal area	-0,657	-67,363	0,001**			
	SE	0,002	3,128	0,002**			
***p < 0,01*							

predictor [11] In 3001 Chinese school children, aged 6 to 19 years, Xiong et al. reported a rapid thinning of the choroid among newly developed myopic patients [17] The results showed that age was positively related to CT for emmetropes and mild myopes greater than −2.00 D. However, there was no significant relationship between age and the CT in children with spherical equivalent less than −2.00 D. Jin et al. observed choroidal thinning during the myopic shift in 118 children aged 7 to 12 years [19] Longer AL and central foveal choroidal thinning were associated with myopic shift, but AL increase was not significantly related to choroidal thinning. They suggested that lack of an association between AL and CT shows the presence of different mechanisms during the development of myopia, and decreased CT may not be a mechanical sequela of globe elongation.

In 96 myopic children (57 girls and 39 boys) between 8 to 15 years, Li et al [28] were the first to report the factors affecting the choroidal structural parameters obtained from the EDI-OCT images. The authors found an association between the LA and AL, and the SA and age. There was no significant association between SE and any choroidal parameter in their study. Wu et al. reported that, in pediatric anisomyopes, eyes with longer AL tend to have decreased choroidal vascularity and choriocapillaris perfusion than the contralateral eyes with shorter AL [29] They included 70 children, 10 to 17 years old; 43 were boys and 27 were girls, and the mean age was 13.1 ± 1.9 years.

In this study, we measured the choroidal structural parameters in 200 myopic children (100 females, 100 males) with a mean age of 11.5 ± 1.6 years. According to the results, contrary to Li et al [28], age and AL were not associated with the LA and the CVI, but SE was significantly associated with the LA and CVI. The disparity between the two studies may be due to the number of patients, age interval, and gender differences, and should be clarified further. Although the exact mechanism of the choroidal changes according to the refractive status is not fully understood in children, the results of our study suggest that refractive error of this age group seems to have a more prominent effect on the vascular structure of the choroid than age-related changes or axial elongation of the eye.

The study had some limitations. It had a cross-sectional design, therefore longitudinal studies should investigate the factors affecting the choroidal structure further. In addition, choroidal blood flow was not measured in the study, therefore combining the technique with OCT-angiography may show more characteristics of the choroidal changes. Changes in choroidal vasculature in myopic children should also be evaluated in different age groups. The strength of our study is the evaluation of the associated factors affecting the choroidal structural parameters and the CVI in a large population of patients with mild to moderate myopia.

The current study demonstrated the structural characteristics of the choroid and their associations in a substantial population of myopic children, which was different from the results of the previous studies. Further studies are needed to support the results of the current study and to elucidate the factors affecting the choroidal structural parameters in myopic children.

CRediT authorship contribution statement

Nazife Aşıkgarip: Writing – original draft, Methodology, Investigation, Formal analysis, Data curation, Conceptualization. **Emine Temel:** Conceptualization, Data curation, Formal analysis, Investigation, Methodology, Resources, Software, Writing – original draft, Writing – review & editing. **Kemal Örnek:** Writing – review & editing, Writing – original draft, Methodology, Investigation, Formal analysis, Data curation, Conceptualization.

Declaration of Competing Interest

The authors declare that they have no conflict of interest.

Acknowledgements

Funding: There are no sources of funding.
The manuscript has been read and approved by all the authors.

References

[1] C.D. Luu, A.M. Lau, S.Y. Lee, Multifocal electroretinogram in adults and children with myopia, Arch. Ophthalmol. 124 (2006) 328–334, https://doi.org/10.1001/archopht.124.3.328.
[2] B.A. Holden, T.R. Fricke, D.A. Wilson, et al., Global prevalence of myopia and high myopia and temporal trends from 2000 through 2050, Ophthalmology 123 (2016) 1036–1042, https://doi.org/10.1016/j.ophtha.2016.01.006.
[3] P.C. Wu, H.M. Huang, H.J. Yu, et al., Epidemiology of myopia, Asia Pac. J. Ophthalmol. (Phila) 5 (2016) 386–393, https://doi.org/10.1097/APO.0000000000000236.
[4] J. Wallman, C. Wildsoet, X.A. Gottlieb, et al., Moving the retina: choroidal modulation of refractive state, Vis. Res. 1 (1995) 37–50, https://doi.org/10.1016/0042-6989(94)e0049-q.
[5] J.A. Summers, The choroid as a sclera growth regulator, Exp. Eye Res. 114 (2013) 120–127, https://doi.org/10.1016/j.exer.2013.03.008.
[6] C.K. Leung, C.Y. Cheung, R.N. Weinreb, et al., Comparison of macular thickness measurements between time domain and spectral domain optical coherence tomography, Invest. Ophthalmol. Vis. Sci. 49 (2008) 4893–4897, https://doi.org/10.1167/iovs.07-1326.
[7] Y. Ikuno, K. Kawaguchi, T. Nouchi, et al., Choroidal thickness in healthy Japanese subjects, Invest. Ophthalmol. Vis. Sci. 51 (2010) 2173–2176, https://doi.org/10.1167/iovs.09-4383.
[8] X. Ding, J. Li, J. Zeng, et al., Choroidal thickness in healthy Chinese subjects, Invest. Ophthalmol. Vis. Sci. 52 (2011) 9555–9560, https://doi.org/10.1167/iovs.11-8076.
[9] X.Q. Li, M. Larsen, I.C. Munch, Subfoveal choroidal thickness in relation to sex and axial length in 93 Danish university students, Invest. Ophthalmol. Vis. Sci. 52 (2011) 8438–8441, https://doi.org/10.1167/iovs.11-8108.
[10] F.K. Chen, J. Yeoh, W. Rahman, et al., Topographic variation and interocular symmetry of macular choroidal thickness using enhanced depth imaging optical coherence tomography, Invest. Ophthalmol. Vis. Sci. 53 (2012) 975–985, https://doi.org/10.1167/iovs.11-8771.
[11] S.A. Read, M.J. Collins, S.J. Vincent, et al., Choroidal thickness in myopic and nonmyopic children assessed with enhanced depth imaging optical coherence tomography, Invest. Ophthalmol. Vis. Sci. 54 (2013) 7578–7586, https://doi.org/10.1167/iovs.13-12772.
[12] S.A. Read, M.J. Collins, S.J. Vincent, et al., Choroidal thickness in childhood, Invest. Ophthalmol. Vis. Sci. 54 (2013) 3586–3593, https://doi.org/10.1167/iovs.13-11732.
[13] M. Bidaut-Garnier, C. Schwartz, M. Puyraveau, et al., Choroidal thickness measurement in children using optical coherence tomography, Retina 34 (2014) 768–774, https://doi.org/10.1097/IAE.0b013e3182a487a4.
[14] A. Bulut, V. Öner, Ş. Büyüktarakçı, et al., Associations between choroidal thickness, axial length and spherical equivalent in a paediatric population, Clin. Exp. Optom. 99 (2016) 356–359, https://doi.org/10.1111/cxo.12353.
[15] P. Gupta, S.G. Thakku, S.M. Saw, et al., Characterization of Choroidal Morphologic and Vascular Features in Young Men With High Myopia Using Spectral-Domain Optical Coherence Tomography, Am. J. Ophthalmol. 177 (2017) 27–33, https://doi.org/10.1016/j.ajo.2017.02.001.
[16] X. Guo, M. Fu, X. Ding, et al., Significant Axial Elongation with Minimal Change in Refraction in 3- to 6-Year-Old Chinese Preschoolers: The Shenzhen Kindergarten Eye Study, Ophthalmology 124 (2017) 1826–1838, https://doi.org/10.1016/j.ophtha.2017.05.030.
[17] S. Xiong, X. He, J. Deng, et al., Choroidal Thickness in 3001 Chinese Children Aged 6 to 19 Years Using Swept-Source OCT, Sci. Rep. 7 (2017) 45059, https://doi.org/10.1038/srep45059.
[18] J. Matalia, N.S. Anegondi, L. Veeboy, et al., Age and myopia associated optical coherence tomography of retina and choroid in pediatric eyes, Indian J. Ophthalmol. 66 (2018) 77–82, https://doi.org/10.4103/ijo.IJO_652_17.
[19] P. Jin, H. Zou, X. Xu, et al., Longitudinal changes in choroidal and retinal thicknesses in children with myopic shift, Retina 39 (2019) 1091–1099, https://doi.org/10.1097/IAE.0000000000002090.
[20] K. Mori, P.L. Gehlbach, S. Yoneya, E.T. AL, Asymmetry of choroidal venous vascular patterns in the human eye, Ophthalmology 11 (2004) 507–512, https://doi.org/10.1016/j.ophtha.2003.06.009.
[21] H. Isono, S. Kishi, Y. Kimura, et al., Observation of choroidal circulation using index of erythrocytic velocity, Arch. Ophthalmol. 121 (2003) 225–231, https://doi.org/10.1001/archopht.121.2.225.
[22] E.D. Cole, E.A. Novais, R.N. Louzada, et al., Contemporary retinal imaging techniques in diabetic retinopathy: a review, Clin. Exp. Ophthalmol. 44 (2016) 289–299, https://doi.org/10.1111/ceo.12711.
[23] G. Calzetti, K. Fondi, A.M. Bata, et al., Assessment of choroidal blood flow using laser speckle flowgraphy, Br. J. Ophthalmol. 102 (12) (2018) 1679–1683, https://doi.org/10.1136/bjophthalmol-2017-311750.
[24] D. Huang, E.A. Swanson, C.P. Lin, et al., Optical Coherence Tomography, Science 254 (1991) 1178–1181, https://doi.org/10.1126/science.1957169.

[25] J.B. Thomsen, B. Sander, M. Mogensen, et al., Optical coherence tomography: technique and applications, Adv. Imaging Biol. Med. Technol. Softw. Environ. 66 (2009) 103–129.
[26] A.G. Podoleanu, Optical coherence tomography, J. Microsc. 247 (2012) 209–219, https://doi.org/10.1111/j.1365-2818.2012.03619.x.
[27] R.F. Spaide, H. Koizumi, M.C. Pozonni, Enhanced depth imaging spectral-domain optical coherence tomography, Am. J. Ophthalmol. 146 (2008) 496–500.
[28] Z. Li, W. Long, Y. Hu, et al., Features of the Choroidal Structures in Myopic Children Based on Image Binarization of Optical Coherence Tomography, Invest. Ophthalmol. Vis. Sci. 61 (2020) 18, https://doi.org/10.1167/iovs.61.4.18.
[29] H. Wu, Z. Xie, P. Wang, et al., Differences in Retinal and Choroidal Vasculature and Perfusion Related to Axial Length in Pediatric Anisomyopes, Invest. Ophthalmol. Vis. Sci. 62 (2021) 40, https://doi.org/10.1167/iovs.62.9.40.
[30] D.L. Nickla, J. Wallman, The multifunctional choroid, Prog. Retin. Eye Res. 29 (2010) 144–168, https://doi.org/10.1016/j.preteyeres.2009.12.002.
[31] L.A. Branchini, M. Adhi, C.V. Regatieri, et al., Analysis of choroidal morphologic features and vasculature in healthy eyes using spectral-domain optical coherence tomography, Ophthalmology 120 (2013) 1901–1908, https://doi.org/10.1016/j.ophtha.2013.01.066.
[32] S. Sonoda, T. Sakamoto, T. Yamashita, et al., Luminal and stromal areas of choroid determined by binarization method of optical coherence tomographic images, Am. J. Ophthalmol. 159 (2015) 1123–1131, https://doi.org/10.1016/j.ajo.2015.03.005.
[33] R. Agrawal, P. Gupta, K.A. Tan, et al., Choroidal vascularity index as a measure of vascular status of the choroid: measurements in healthy eyes from a population-based study, Sci. Rep. 6 (2016) 21090, https://doi.org/10.1038/srep21090.
[34] R. Agrawal, J. Chhablani, K.-A. Tan, et al., Choroidal vascularity index in central serous chorioretinopathy, Retina 36 (2016) 1646–1651, https://doi.org/10.1097/IAE.0000000000001040.
[35] R. Agrawal, L.K.H. Li, V. Nakhate, et al., Choroidal vascularity index in Vogt-Koyanagi-Harada disease: an EDI-OCT derived tool for monitoring disease progression, Trans. Vis. Sci. Tech. 5 (2016) 7, https://doi.org/10.1167/tvst.5.4.7.
[36] R. Agrawal, M. Salman, K.-A. Tan, et al., Choroidal vascularity index (CVI)-a novel optical coherence tomography parameter for monitoring patients with panuveitis? PLoS One 11 (2016), e0146344 https://doi.org/10.1371/journal.pone.0146344.
[37] X. Wei, D.S.W. Ting, W.Y. Ng, et al., Choroidal vascularity index: a novel optical coherence tomography based parameter in patients with exudative age-related macular degeneration, Retina 37 (2017) 1120–1125, https://doi.org/10.1097/IAE.0000000000001312.